Identification of SLURP-1 as an epidermal neuromodulator explains the clinical phenotype of Mal de Meleda

Fabrice Chimienti[1], Ronald C. Hogg[2], Laure Plantard[1], Caroline Lehmann[1], Noureddine Brakch[3], Judith Fischer[4], Marcel Huber[1], Daniel Bertrand[2] and Daniel Hohl[1,*]

[1]Laboratory for Cutaneous Biology, Dermatology Unit, CHUV, Lausanne, Switzerland, [2]Department of Physiology, CMU, Geneva, Switzerland, [3]Division of Hypertension and Vascular Medicine, CHUV, Lausanne, Switzerland and [4]Centre National de Génotypage, Evry, France

Mal de Meleda is an autosomal recessive inflammatory and keratotic palmoplantar skin disorder due to mutations in the *ARS B* gene, encoding for SLURP-1 (secreted mammalian Ly-6/uPAR-related protein 1). SLURP-1 belongs to the Ly-6/uPAR superfamily of receptor and secreted proteins, which participate in signal transduction, immune cell activation or cellular adhesion. The high degree of structural similarity between SLURP-1 and the three fingers motif of snake neurotoxins and Lynx1 suggests that this protein interacts with the neuronal acetylcholine receptors. We found that SLURP-1 potentiates the human α7 nicotinic acetylcholine receptors that are present in keratinocytes. These results identify SLURP-1 as a secreted epidermal neuromodulator which is likely to be essential for both epidermal homeostasis and inhibition of TNF-alpha release by macrophages during wound healing. This explains both the hyperproliferative as well as the inflammatory clinical phenotype of Mal de Meleda.

INTRODUCTION

Mal de Meleda (MdM, OMIM 284300, syn. keratosis palmoplantaris transgrediens of Siemens), is an autosomal recessive palmoplantar keratoderma originally described in patients from the island of Meleda, Croatia (1). It is characterized by an inflammatory, malodorous, sharply demarcated, palmoplantar keratoderma, involving palms and soles and extending on ('transgressing') the back of hands and feet as well as the wrists and heels. Frequently associated features are hyperhidrosis, perioral erythema and lichenoid or keratotic plaques over joints, brachydactyly with cone-shaped fingers and nail abnormalities such as koilonychia or pachyonychia (2). The Mal de Meleda gene is located on chromosome 8q24.3 within a cluster of Ly-6 homologous human genes (3), and mutations in the *ARS B* gene, encoding for SLURP-1 (secreted mammalian Ly-6/uPAR-related protein 1), were found to underlie the disease in over 25 unrelated incidences (4–6).

The Ly-6/uPAR superfamily of receptor and secreted proteins contains a carboxy-terminal consensus sequence motif CCXXXXCN and one or several repeats of the Ly-6/uPAR domain, which is defined by a distinct disulfide bonding pattern between eight or 10 cysteine residues (7–9). They can be classified into two subfamilies on the basis of the presence or absence of a GPI-anchoring signal sequence (10). GPI-anchored Ly-6/uPAR receptor proteins include the retinoic acid-induced gene E (RIG-E, or human Ly-6E), the E48 antigen (human Ly-6D), Ly-6H, the PSCA, CD59 or protectin, lynx1 and uPAR (11–15). The E48 gene is known to be expressed in human keratinocytes, but not in lymphocytes, and modulates desmosomal cell–cell adhesion of keratinocytes (12,16). The urokinase-type plasminogen activator receptor (uPAR) interacts in dynamic association with integrins and initiates signaling events that alter cell adhesion, migration, proliferation and differentiation (for review see 17). uPAR is a distant Ly-6/uPAR family member and, contrary to other members, contains three contiguous copies of the Ly-6/uPAR domain, differential cleavage of which regulates its multiple functions (18,19). The second subfamily with a Ly-6/uPAR domain but no GPI-anchoring signal sequence includes SLURP-1, a 9 kDa protein encoded by the *ARS B* gene and the recently reported SLURP-2 (10,20). Phylogenetic analysis

*To whom correspondence should be addressed at: Laboratory for Cutaneous Biology, Dermatology Unit, Beaumont Hospital, CHUV-BT 437, CH-1011 Lausanne, Switzerland. Tel: +41 213140353; Fax: +41 213140382; Email: daniel.hohl@hospvd.ch

based on the SLURP-1 primary protein structure revealed a close relationship to the subfamily of single-domain snake and frog cytotoxins, i.e. α-bungarotoxin (Bgtx) and α-cobratoxin (Cbtx). Thus, SLURP-1 is expected to fold similarly to the snake neurotoxins (21) and contains a signal peptide (amino acids 1–22), suggesting that it could be secreted. Although it has been shown that mutations of SLURP-1 are implicated in MdM, its molecular function remained unknown. SLURP-1 may function as a ligand for a receptor yet to be identified, e.g. in intercellular adhesion as has been shown for E48 (Ly-6D) and its ligand Ly-6D-L (22).

The high degree of structural homology between SLURP-1 and the snake neurotoxins suggests that it may interact with ion channels, in a way comparable to the action of Lynx1, a GPI-anchored Ly-6/uPAR protein with structural and functional similarity to snake venom toxins. Lynx1 has been shown to interact with neuronal nicotinic acetylcholine receptors in the central nervous system where it modulates the cellular calcium permeability (23). α7 nicotinic receptors have been reported to play a central role in the differentiation of stratified squamous epithelium (24).

In this study we isolated, purified and characterized the SLURP-1 protein. We demonstrate that SLURP-1 is secreted by N-terminal signal cleavage and acts as a neuromodulator of the α7 nicotinic receptor (α7 nAChR), suggesting that it may regulate epidermal calcium homeostasis and cutaneous inflammation.

RESULTS

SLURP-1 is a propeptide cleaved prior to secretion

To assess whether SLURP-1 is indeed secreted and to test for the actual presence of the putative cleavage site of the signal sequence, we produced recombinant protein SLURP-1 with an N-terminal haemaglutinin (HA) tag and a C-terminal myc tag (Fig. 1A). After transient transfection of 293T cells we identified SLURP-1 48 h later in the culture medium by immunoblotting with anti-myc antibodies. The absence of the HA-tagged protein (Fig. 1B) suggests that SLURP-1 is cleaved before secretion.

We purified recombinant polyhistidine-tagged SLURP-1 by a cobalt affinity chromatography with Talon resin (Clontech). Most proteins did not bind the resin, and remained in the flow-through fraction (Fig. 2A). We eliminated co-purified proteins by gel filtration (BioRad BioPrepSE-100/17) to obtain pure recombinant SLURP-1 (Fig. 2B). The estimated final yield was about 100 μg of protein per liter of culture medium.

SLURP-1 is a non-glycosylated protein

SLURP-1 contains a putative N-glycosylation site on N64. Since glycosylation could change biological properties, we incubated partially purified SLURP-1 produced in mammalian and insect cells (not shown) with N-glycosidase F, which hydrolyses N-glycan chains. Contaminating proteins were used as internal positive control. The shift in the migration in some of these proteins indicates the proper functioning of the enzyme. This condition does not modify the migration of

SLURP-1 (Fig. 1C), indicating that SLURP-1 is not glycosylated. However the method used is based on a shift in molecular weight of the protein, and thus may not detect glycosylation from a single residue.

SLURP-1 can modulate nicotinic acetylcholine function *in vitro*

Phylogenetic analysis based on the SLURP-1 amino acid sequence reveals a close relationship to the subfamily of single-domain snake and frog cytotoxins, i.e. α-bungarotoxin (Figs 3A and 5). Three-dimensional structure analysis of SLURP-1 suggests that this protein may resemble that of other Ly-6 proteins and three fingered frog and snake venom toxins, i.e. CD59 and α-bungarotoxin (Fig. 3B). To test whether SLURP-1 might be functionally homologous to the venom toxins and act on nAChRs, we examined ACh-elicited macroscopic current responses in control and SLURP-1-treated *Xenopus* oocytes expressing recombinant human α7 nAChRs (Fig. 4). We measured ACh-evoked responses before and after exposure (2.5–5 min) to highly purified SLURP-1. SLURP-1 enhanced the amplitude of the ACh-evoked macroscopic currents in a concentration-dependent manner. At a concentration of 200 pM, SLURP-1 increased the amplitude of the ACh-evoked macroscopic currents by $421 \pm 130\%$ ($n = 6$), and 20 nM SLURP-1 enhanced the amplitude by $1214 \pm 550\%$ ($n = 4$), compared with control (Fig. 4A). SLURP-1 applications exhibited similar activity with all the ACh concentrations tested, except 10 μM. The dose–response curve indicates that SLURP-1 potentiates α7 nAChR homopentamers, since the EC_{50} was 175 μM ACh for the controls and dropped to 68 μM ACh after SLURP-1 treatment (Fig. 4B). The effects of SLURP-1 on the ACh dose–response curve indicate that 200 pM causes an increase in both current amplitude and sensitivity to ACh as well as an increase in the Hill coefficient. Application of SLURP-1 did not evoke currents in the absence of ACh. Thus, SLURP-1 functions not as a ligand or neurotransmitter, but modulates receptor function in the presence of its natural ligand in a manner consistent with an allosteric mode of action.

DISCUSSION

The association between the keratotic palmoplantar skin disorder called Mal de Meleda and mutations in SLURP-1 suggests that alteration of this secreted protein may disrupt the homeostasis of the skin. Additionally, SLURP-1 modification could modify the secretion from macrophages of TNF-α, a pleiotropic cytokine factor that has been shown to elicit inflammatory responses.

The high degree of structural similarity between SLURP-1 and the three-fingered protein family, and the expression of α7 nicotinic acetylcholine receptors in keratinocytes, as well as the role of these receptors in macrophage secretion, point to a possible role of SLURP-1 at this specific ligand-gated channel. Secreted snake α-neurotoxins are known to interact with the muscle and neuronal subtypes of the nicotinic acetylcholine receptor (nAChR), and both muscarinic and nicotinic AChRs are expressed in keratinocytes (25,26). Epidermal nAChRs are involved in regulating cell adhesion and motility of epidermal keratinocytes (27), and nicotine exerts inhibitory effects on keratinocyte migration. nAChRs have been demonstrated to
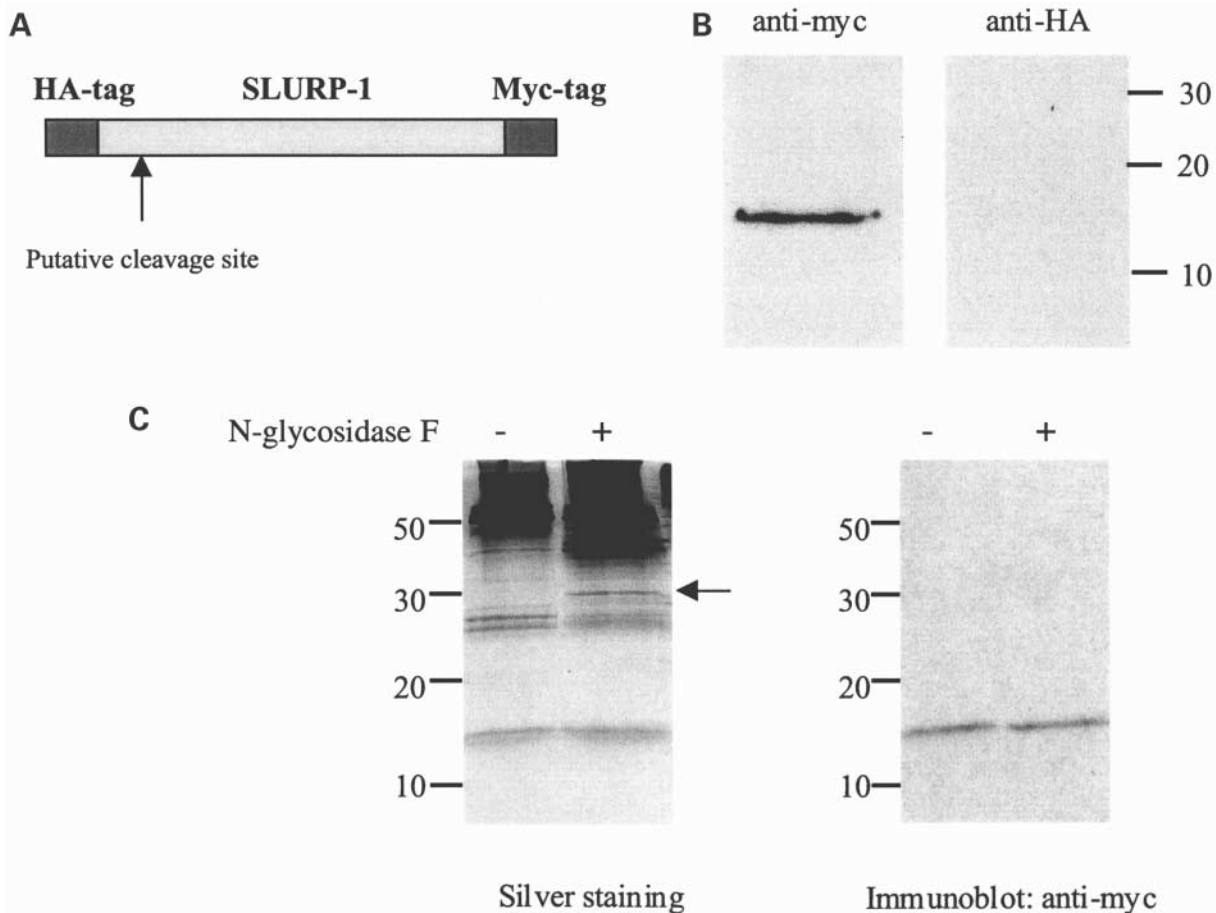
Figure 1. SLURP-1 is a non-glycosylated protein whose signal sequence of SLURP-1 is cleaved during processing. (**A**) SLURP-1 construct tagged with HA-tag in N-terminus and myc-tag in C-terminus, respectively. (**B**) Culture medium was collected after 24 h and directly immunoblotted with anti-myc or anti-HA antibodies. The presence of a myc-tagged protein but not HA-tagged in the culture medium suggests that the signal sequence is cleaved during intracellular processing. (**C**) After N-glycosidase treatment, as described in Methods, proteins are loaded on SDS–PAGE and revealed either by silver staining or immunoblotted with anti-myc antibody. Arrows indicate co-purified deglycosylated protein not present before N-glycosidase treatment.

play a role in wound healing (28). The effects of nicotine may be mediated by $\alpha3$ and $\alpha7$ nAChRs with Ca^{2+} serving as a second messenger in this signaling pathway (29). Calcium has an established role in the homeostasis of mammalian skin, and a gradient of calcium concentration increasing from the basal layer to the stratum granulosum modulates keratinocyte proliferation and differentiation (30,31). Recent data revealed that homomeric $\alpha7$ nAChRs actively participate in the control of epidermal differentiation. Indeed, elimination of the $\alpha7$ signaling pathway was reported to block nicotine-induced influx of $^{45}Ca^{2+}$ and to inhibit expression of markers of epidermal differentiation (24). Thus, ACh signaling through $\alpha7$ nAChR channels appears to be functional in keratinocytes and essential for epidermal homeostasis. TNF-α is a pleiotropic proinflammatory cytokine that elicits a large number of biological effects, including inflammatory and immunoregulatory responses (32). TNF-α is known to be released from keratinocytes after stimulation with lipopolysaccharide (LPS), ultraviolet (UV) light or wound healing and participates in cutaneous inflammation (33). In turn, upon stimulation with proinflammatory cytokines such as TNF-α and IL-1,

keratinocytes synthesize and release LARC/CCL20, which attract CCR6-expressing immature dendritic cells and memory/ effector T cells into the dermis of inflamed skin (34). Macrophages play a significant role in skin inflammation, since they release TNF-α after activation, thereby amplifying the inflammation regulatory loop. ACh inhibits the release of TNF-α and other cytokines on primary macrophages, through a mechanism dependent on bungarotoxin-sensitive receptors (35). The $\alpha7$ nAChR subunit is required for inhibition of TNF-α release by macrophages (36), and inactivation of this pathway can contribute to excessive systemic release of cytokines during endotoxaemia or other injury.

In this study, we identify SLURP-1 as a novel modulator of the human $\alpha7$ nicotinic acetylcholine receptor. The lack of action of SLURP-1 alone and its important potentiation of the agonist response suggests that SLURP-1 acts as a positive allosteric effector at the $\alpha7$ receptor. This hypothesis is further supported by the increased ACh sensitivity and increased apparent cooperativity that are hallmark of allosteric effectors (37). While it remains to be demonstrated that point mutations observed in SLURP-1 disrupt its effect at the $\alpha7$ receptor, other
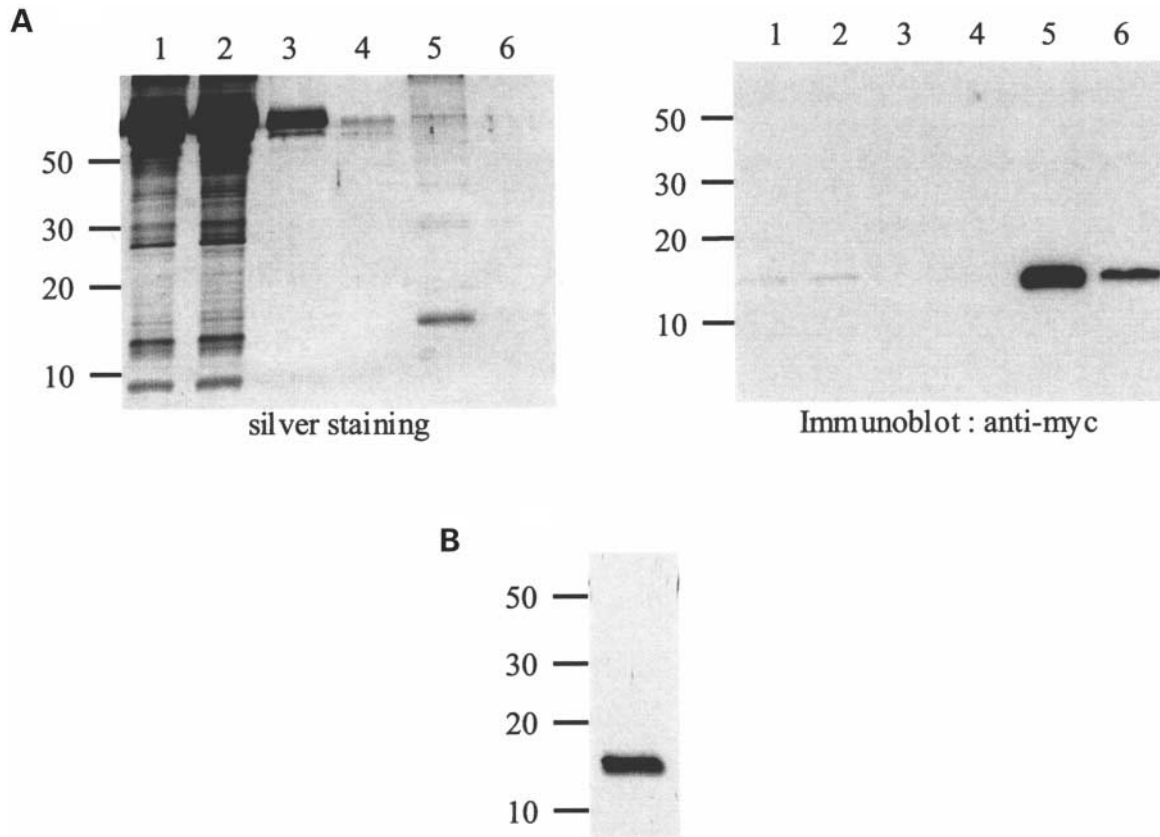
Figure 2. Purification of SLURP-1 from culture medium. (**A**) 293T-SLURP-1 stable cell line were generated by calcium phosphate transfection and Zeocin selection. Culture medium was collected after 72 h. His6-tagged SLURP-1 was purified from culture medium with Talon resin. Fractions were loaded on a 15% SDS–PAGE. Proteins were revealed either by silver staining or immunoblotted with anti-myc antibody. Lane 1, input; lane 2, flow-through; lane 3, wash 1; lane 4, wash 2; lane 5, elution 1; lane 6, elution 2. (**B**) Silver stained SDS–PAGE (15% acrylamide) of recombinant SLURP-1 following purification with Talon resin and size exclusion chromatography.

variants such frame shifts mutations will certainly result in truncated, misfolded and therefore non-functional proteins. Since Mal de Meleda is characterized by a clinical phenotype with marked cutaneous inflammation and is due to absent or mutated SLURP-1, this raises the possibility that SLURP-1 controls TNF-α release in dermal macrophages and in keratinocytes by activation of nAChRs and thus reduced inflammation. The identification of SLURP-1 as a modulator of nAChRs will allow to further define the role of secreted Ly-6 proteins, i.e. SLURP-1 and SLURP-2 in epidermal homeostasis and cutaneous inflammation.

MATERIALS AND METHODS

Plasmid constructions

For expression in mammalian cells, the cDNA encoding for SLURP-1 was modified by PCR to add 5′*Hind*III and 3′*Xba*I restriction sites at their termini with the following primers: sense, 5′-AAGCTTGGAGCAATGGCCTCTCGCTGG and antisense, 5′-TCTAGAGAGTTCCGAGTTGCAGAGGTC. The PCR fragments were purified from agarose gels and ligated into *Hind*III- and *Xba*I-digested pBudCE4 (Invitrogen) to give the plasmid pBud-SLURP-1, which allowed addition of a C-terminal myc tag for detection by western analysis and His$_6$ tag for purification. To generate the recombinant SLURP-1 protein with tags at both N- and C-termini, the cDNA encoding for SLURP-1 was amplified from pBud-SLURP-1 by PCR using primers containing 5′*EcoR*V and 3′*Bgl*II restriction sites at their termini and including the myc tag. The following primers were used: sense, 5′-GAGATATCGGAGCAATGGCC-TCTCG and antisense, 5′-AGAGATCTTCACAGATCCTCTT-CTGAGATG AGTTT. The PCR fragments were purified from agarose gels and ligated into *EcoR*V- and *Bgl*II-digested pCRUZ-HA (Santa Cruz), to generate pCSLURP-1, which allowed addition of an N-terminal haemagglutinin (HA) tag (see Fig. 2).

The resulting plasmids were then used to transform competent XL1-Blue cells. Single colonies were picked, and plasmid DNA was isolated and purified using reagents from Qiagen according to the manufacturer's instructions. For expression in insect cells, the pBud-SLURP-1 plasmid was digested by *Hind*III and *EcoR*V. The fragment corresponding to SLURP-1 cDNA with a myc tag at C-terminus was purified from agarose gels and ligated into *Hind*III- and *Xba*I-digested pIZ (Invitrogen), thus generating pIZ-SLURP-1, which encodes for the same protein as pBud-SLURP-1, including
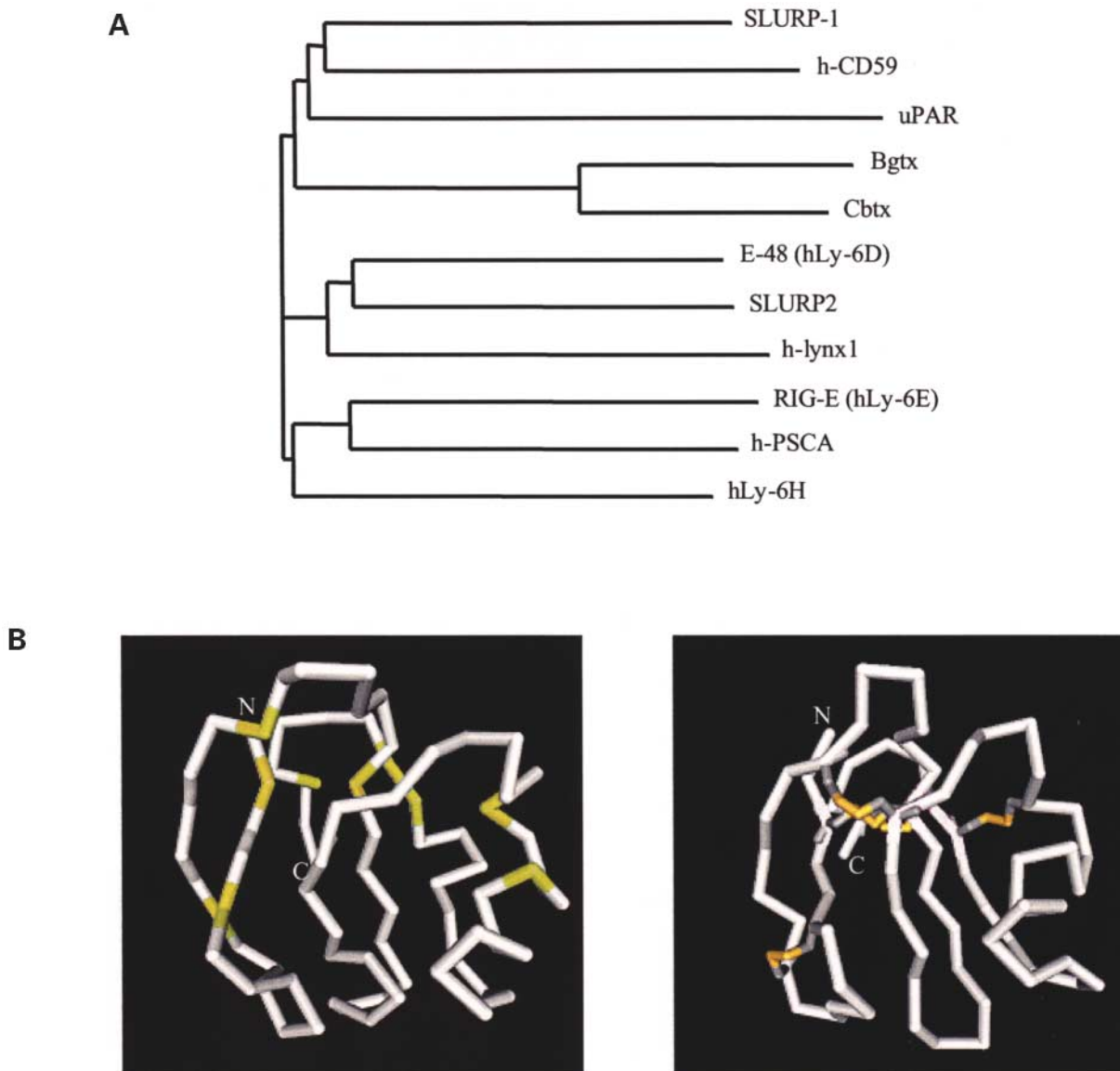
Figure 3. SLURP-1 is member of the Ly6/αBgtx families. (**A**) Phylogenetic tree of the Ly6/αBgtx families showing the relationship between secreted snake toxins and the GPI-anchored Ly6/uPAR family. SLURP-1 is phylogenetically more closely related to snake toxins than it is to the mammalian GPI-anchored receptors. Phylogenetic tree calculation is based on a sequence distance method and utilizes the neighbor joining algorithm (41). (**B**) Comparison of the SLURP-1 model (left) and the CD59 extracellular domain experimental NMR structure (right, PDB code: 1ERG). SLURP-1 cysteines are colored in yellow, as disulfide bridges of the CD59 extracellular domain. Note the homologous disposition of CD59 disulfide bridges and SLURP-1 cysteines. Both proteins structurally adopt, or are predicted to adopt, the characteristic 'three-finger' appearance of snake proteins. N- and C-terminal ends of the molecules are labeled.

myc and His$_6$ tags. Correct insertion and in frame cloning of all plasmids was verified by sequencing.

Cell lines

HEK 293T cells (ATCC CRL-11268) were cultured in Dulbecco's modified Eagle's medium supplemented with 10% fetal calf serum (Gibco), 2 mM L-glutamine, 100 units/ml penicillin, and 100 µg/ml streptomycin, at 37°C in a 5% CO$_2$ humidified atmosphere. The cells were harvested by trypsinization when ~90% confluent and plated at split ratios of 1 : 5. Stable cell lines expressing SLURP-1 were generated by calcium phosphate transfection of pBud-SLURP-1 as previously described (38) and Zeocin selection. Clonal cell lines were isolated by the dilution method. *Trichoplusia ni* (HighFive, Invitrogen) cells were maintained at 27°C in Express Five® SFM medium (Life Technologies). To generate stable cell lines, 10 µg of pIZ-SLURP-1 was transfected in HighFive cells with Cellfectin™ according to the manufacturer's instructions. Zeocin was added 48 h later for selection. Clonal cell lines were isolated with cloning cylinders.

Purification of recombinant SLURP-1

Recombinant SLURP-1 was purified using the His$_6$ tag from the culture medium of stably transfected mammalian and insect

A

B

C
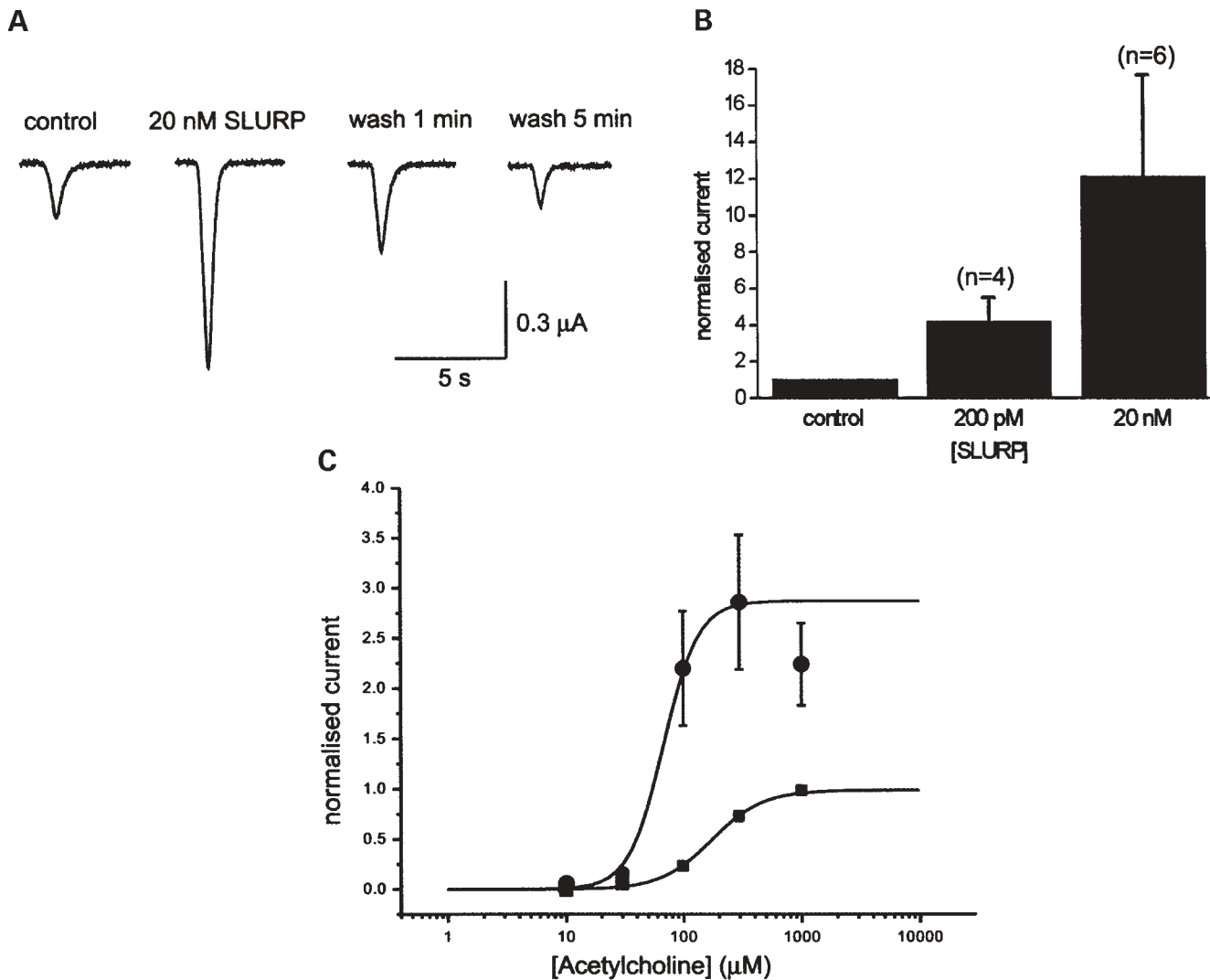
Figure 4. SLURP-1 can modulate nicotinic acetylcholine function *in vitro*. (**A**) Current responses before and after 5 min exposure to 20 nM SLURP-1. Currents were activated by a 2s application of 100 μM ACh. (**B**) Effects of SLURP-1 are concentration-dependant, currents were activated by 200 or 300 μM ACh. (**C**) 200 pM SLURP-1 shifted the ACh dose response curve (closed squares) to the left and increased E_{max} (solid circles). EC_{50} was 178 μM for control and 68 μM after 2.5 min exposure to SLURP-1 (200 pM). $n = 6$ for each data point.

cells, which were cultured for 3 days before the medium was harvested. After dialysis against buffer A (50 mM sodium phosphate; 300 mM NaCl; pH 7.4), supernatants were incubated with Talon resin (Clontech) and the native buffer protocol provided. After washing, the fusion protein was eluted with buffer A containing 150 mM imidazole. The fractions containing SLURP-1 were either dialysed against buffer A or loaded on a BioRad BioPrepSE-100/17gel filtration chromatography column and eluted with buffer A to obtain pure recombinant SLURP-1.

Treatment with N-glycosidase F

Approximately 10 μg of myc-His$_6$-tagged SLURP-1 partially purified either from insect or mammalian cells culture medium was diluted in a solution of 25 mM sodium phosphate (pH 7.0), 25 mM EDTA, and 0.15% SDS and then heated at 100°C for
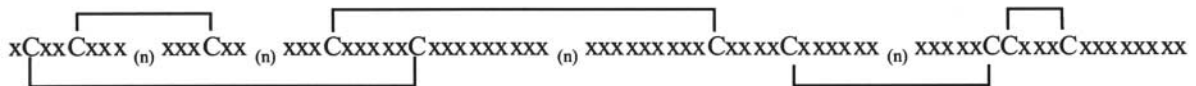
5 min. After the solution cooled, 10% Nonidet P-40 and 0.6U N-glycosidase F (Roche) were added (final detergent concentrations, 0.1% SDS and 0.5% Nonidet P-40) and the mixture was incubated at 37°C for 20 h. The reaction was stopped by adding SDS–PAGE sample buffer, followed by incubation at 100°C for 5 min. Samples were then loaded in 15% SDS–PAGE and revealed with silver staining or western blotting, using co-purified proteins as internal positive control for N-glycosidase F activity.

Structural modeling

Three dimensional model of SLURP-1 was built by the computer program 3D-PSSM (39) (www.sbg.bio.ic.ac.uk/srvers/3dpssm). 3D-PSSM (three-dimensional position-specific scoring matrix) uses structural alignments of homologous proteins of similar three-dimensional structure in the structural
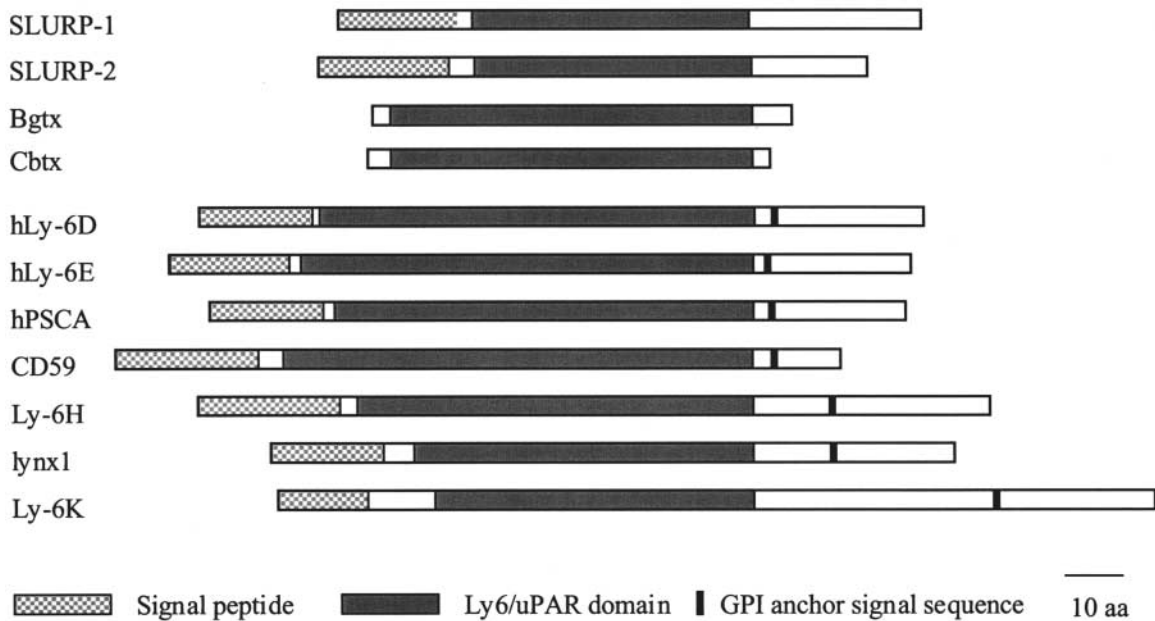
Figure 5. Comparison of domain constitution between members of the Ly-6/uPAR family and snake venom toxins. All the proteins of the family share the same consensus domain (Prosite acc number PS00983, see below). uPAR shares the same structure but contains three contiguous Ly6/uPAR domains (not shown). The GPI anchor signal sequence indicates cleavage site after addition of GPI moiety.

classification of proteins (SCOP) database to obtain a structural equivalence of residues. These equivalences are used to extend multiply aligned sequences obtained by standard sequence searches. The resulting large superfamily-based multiple alignment is converted into a PSSM. Combined with secondary structure matching and solvation potentials, 3D-PSSM can recognize structural and functional relationships between homologous proteins (39).

Oocyte preparation and injection

X. laevis oocytes were isolated and prepared as described previously (40). Oocytes were intranuclearly injected with 2 ng of human α7 cDNA and kept in separate wells of a 96-well microtitre plate at 18°C. OR2 control medium consisted of 88 mM NaCl, 2.5 mM KCl, 10 mM HEPES, 1 mM $MgCl_2$, and 2 mM $CaCl_2$, pH 7.4, adjusted with NaOH.

Electrophysiology

Experiments were carried out 2–4 days after cDNA injection. Electrophysiological recordings were performed using a two-electrode voltage-clamp (GeneClamp amplifier; Axon Instruments, Union City, CA, USA); holding potential was −100 mV. Electrodes were pulled from borosilicate glass and contained 3 M KCl. Solution exchanges were performed by an automated system based around a liquid handling robot. Oocytes were continuously superfused with OR2 except during peptide incubation. Oocytes were maintained at 18°C during experiments. Dose–response curves were fit by the equation $y = I_{max} * \{1/(1 + (EC_{50}/[ACh])^n)\}$, where I_{max} is the maximal normalized current amplitude, EC_{50} the half effective agonist concentration, n the Hill coefficient and [ACh] the ACh concentration.

REFERENCES

1. Neumann, I. (1898) Ueber Keratoma Hereditarium. *Arch. Derm. Syph.*, **42**, 163–174.
2. Franceschetti, A.T., Reinhart, V. and Schnyder U.W. (1972) Meleda disease. *J. Genet. Hum.*, **20**, 267–296.

3. Fischer, J., Bouadjar, B., Heilig, R., Fizames, C., Prud'homme, J.F. and Weissenbach, J. (1998) Genetic linkage of Meleda disease to chromosome 8qter. *Eur. J. Hum. Genet.*, **6**, 542–547.

4. Fischer, J., Bouadjar, B., Heilig, R., Huber, M., Lefevre, C., Jobard, F., Macari, F., Bakija-Konsuo, A., Ait-Belkacem, F., Weissenbach, J. *et al.* (2001) Mutations in the gene encoding SLURP-1 in Mal de Meleda. *Hum. Mol. Genet.*, **10**, 875–880.

5. Eckl, K.M., Stevens, H.P., Lestringant, G.G., Westenberger-Treumann, M., Traupe, H., Hinz, B., Frossard, P.M., Stadler, R., Leigh, I.M., Nurnberg, P. *et al.* (2003) Mal de Meleda (MDM) caused by mutations in the gene for SLURP-1 in patients from Germany, Turkey, Palestine, and the United Arab Emirates. *Hum. Genet.*, **112**, 50–56.

6. Ward, K.M., Yerebakan, O., Yilmaz, E. and Celebi, J.T. (2003) Identification of recurrent mutations in the ARS (Component B) gene encoding SLURP-1 in two families with Mal de Meleda. *J. Invest. Dermatol.*, **120**, 96–98.

7. Ploug, M., Kjalke, M., Ronne, E., Weidle, U., Hoyer-Hansen, G. and Dano, K. (1993) Localization of the disulfide bonds in the NH2-terminal domain of the cellular receptor for human urokinase-type plasminogen activator. A domain structure belonging to a novel superfamily of glycolipid-anchored membrane proteins. *J. Biol. Chem.*, **268**, 17539–17546.

8. Ploug, M. and Ellis, V. (1994) Structure-function relationships in the receptor for urokinase-type plasminogen activator. Comparison to other members of the Ly-6 family and snake venom alpha-neurotoxins. *FEBS Lett.*, **349**, 163–168.

9. Casey, J.R., Petranka, J.G., Kottra, J., Fleenor, D.E. and Rosse, W.F. (1994) The structure of the urokinase-type plasminogen activator receptor gene. *Blood*, **84**, 1151–1156.

10. Adermann, K., Wattler, F., Wattler, S., Heine, G., Meyer, M., Forssmann, W.G. and Nehls, M. (1999) Structural and phylogenetic characterization of human SLURP-1, the first secreted mammalian member of the Ly-6/uPAR protein superfamily. *Protein Sci.*, **8**, 810–819.

11. Shan, X., Bourdeau, A., Rhoton, A., Wells, D.E., Cohen, E.H., Landgraf, B.E. and Palfree, R.G. (1998) Characterization and mapping to human chromosome 8q24.3 of Ly-6-related gene 9804 encoding an apparent homologue of mouse TSA-1. *J. Immunol.*, **160**, 197–208.

12. Brakenhoff, R.H., Gerretsen, M., Knippels, E.M., van Dijk, M., van Essen, H., Weghuis, D.O., Sinke, R.J., Snow, G.B. and van Dongen, G.A. (1995) The human E48 antigen, highly homologous to the murine Ly-6 antigen ThB, is a GPI-anchored molecule apparently involved in keratinocyte cell–cell adhesion. *J. Cell Biol.*, **129**, 1677–1689.

13. Horie, M., Okutomi, K., Taniguchi, Y., Ohbuchi, Y., Suzuki, M. and Takahashi, T. (1998) Isolation and characterization of a new member of the human Ly6 gene family (LY6H). *Genomics*, **53**, 365–368.

14. Reiter, R.E., Gu, Z., Watabe, T., Thomas, G., Szigeti, K., Davis, E., Wahl, M., Nisitani, S., Yamashiro, J., Le Beau, M.M. *et al.* (1998) Prostate stem cell antigen: a cell surface marker overexpressed in prostate cancer. *Proc. Natl Acad. Sci. USA*, **95**, 1735–1740.

15. Tone, M., Walsh, L.A. and Waldmann, H. (1992) Gene structure of human CD59 and demonstration that discrete mRNAs are generated by alternative polyadenylation. *J. Mol. Biol.*, **227**, 971–976.

16. Schrijvers, A.H., Gerretsen, M., Fritz, J.M., van Walsum, M., Quak, J.J., Snow, G.B. and van Dongen, G.A. (1991) Evidence for a role of the monoclonal antibody E48 defined antigen in cell–cell adhesion in squamous epithelia and head and neck squamous cell carcinoma. *Exp. Cell. Res.*, **196**, 264–269.

17. Blasi, F. and Carmeliet, P. (2002) uPAR: a versatile signalling orchestrator. *Nat. Rev. Mol. Cell. Biol.*, **3**, 932–943.

18. Palfree, R.G. (1991) The urokinase-type plasminogen activator receptor is a member of the Ly-6 superfamily. *Immunol. Today*, **12**, 170.

19. Montuori, N., Carriero, M.V., Salzano, S., Rossi, G. and Ragno, P. (2002) The cleavage of the urokinase receptor regulates its multiple functions. *J .Biol. Chem.*, **277**, 46932–46939.

20. Tsuji, H., Okamoto, K., Matsuzaka, Y., Iizuka, H., Tamiya, G. and Inoko,H. (2003) SLURP-2, a novel member of the human Ly-6 superfamily that is up-regulated in psoriasis vulgaris (small star, filled). *Genomics*, **81**, 26–33.

21. Tsetlin, V. (1999) Snake venom alpha-neurotoxins and other 'three-finger' proteins. *Eur. J. Biochem.*, **264**, 281–286.

22. Apostolopoulos, J., McKenzie, I.F. and Sandrin, M.S. (2000) Ly6d-L, a cell surface ligand for mouse Ly6d. *Immunity*, **12**, 223–232.

23. Miwa, J.M., Ibanez-Tallon, I., Crabtree, G.W., Sanchez, R., Sali, A., Role, L.W. and Heintz, N. (1999) lynx1, an endogenous toxin–like modulator of nicotinic acetylcholine receptors in the mammalian CNS. *Neuron*, **23**, 105–114.

24. Arredondo, J., Nguyen, V.T., Chernyavsky, A.I., Bercovich, D., Orr-Urtreger, A., Kummer, W., Lips, K., Vetter, D.E. and Grando, S.A. (2002) Central role of {alpha}7 nicotinic receptor in differentiation of the stratified squamous epithelium. *J. Cell Biol.*, **21**, 21.

25. Grando, S.A. and Horton, R.M. (1997) The keratinocyte cholinergic system with acetylcholine as an epidermal neurotransmitter. *Curr. Opin. Dermatol.*, **4**, 262–268.

26. Grando, S.A. (1997) Biological functions of keratinocyte cholinergic receptors. *J. Invest. Dermatol. Symp. Proc.*, **2**, 41–48.

27. Grando, S.A., Horton, R.M., Pereira, E.F., Diethelm-Okita, B.M., George, P.M., Albuquerque, E.X. and Conti-Fine, B.M. (1995) A nicotinic acetylcholine receptor regulating cell adhesion and motility is expressed in human keratinocytes. *J. Invest. Dermatol.*, **105**, 774–781.

28. Jacobi, J., Jang, J.J., Sundram, U., Dayoub, H., Fajardo, L.F. and Cooke, J.P. (2002) Nicotine accelerates angiogenesis and wound healing in genetically diabetic mice. *Am. J. Pathol.*, **161**, 97–104.

29. Zia, S., Ndoye, A., Lee, T.X., Webber, R.J. and Grando, S.A. (2000) Receptor-mediated inhibition of keratinocyte migration by nicotine involves modulations of calcium influx and intracellular concentration. *J. Pharmacol. Exp. Ther.*, **293**, 973–981.

30. Menon, G.K., Grayson, S. and Elias, P.M. (1985) Ionic calcium reservoirs in mammalian epidermis: ultrastructural localization by ion-capture cytochemistry. *J. Invest. Dermatol.*, **84**, 508–512.

31. Elias, P.M., Ahn, S.K., Denda, M., Brown, B.E., Crumrine, D., Kimutai, L.K., Komuves, L., Lee, S.H. and Feingold, K.R. (2002) Modulations in epidermal calcium regulate the expression of differentiation-specific markers. *J. Invest. Dermatol.*, **119**, 1128–1136.

32. Kondo, S. and Sauder, D.N. (1997) Tumor necrosis factor (TNF) receptor type 1 (p55) is a main mediator for TNF-alpha-induced skin inflammation. *Eur. J. Immunol.*, **27**, 1713–1718.

33. Kock, A., Schwarz, T., Kirnbauer, R., Urbanski, A., Perry, P., Ansel, J.C. and Luger, T.A. (1990) Human keratinocytes are a source for tumor necrosis factor alpha: evidence for synthesis and release upon stimulation with endotoxin or ultraviolet light. *J. Exp. Med.*, **172**, 1609–1614.

34. Nakayama, T., Fujisawa, R., Yamada, H., Horikawa, T., Kawasaki, H., Hieshima, K., Izawa, D., Fujiie, S., Tezuka, T. and Yoshie, O. (2001) Inducible expression of a CC chemokine liver- and activation-regulated chemokine (LARC)/macrophage inflammatory protein (MIP)-3 alpha/ CCL20 by epidermal keratinocytes and its role in atopic dermatitis. *Int. Immunol.*, **13**, 95–103.

35. Borovikova, L.V., Ivanova, S., Zhang, M., Yang, H., Botchkina, G.I., Watkins, L.R., Wang, H., Abumrad, N., Eaton, J.W. and Tracey, K.J. (2000) Vagus nerve stimulation attenuates the systemic inflammatory response to endotoxin. *Nature*, **405**, 458–462.

36. Wang, H., Yu, M., Ochani, M., Amella, C.A., Tanovic, M., Susarla, S., Li, J.H., Yang, H., Ulloa, L., Al-Abed, Y. *et al.* (2003) Nicotinic acetylcholine receptor alpha7 subunit is an essential regulator of inflammation. *Nature*, **421**, 384–388.

37. Changeux, J. and Edelstein, S.J. (2001) Allosteric mechanisms in normal and pathological nicotinic acetylcholine receptors. *Curr. Opin. Neurobiol.*, **11**, 369–377.

38. Jordan, M., Schallhorn, A. and Wurm, F.M. (1996) Transfecting mammalian cells: optimization of critical parameters affecting calcium-phosphate precipitate formation. *Nucl. Acids Res.*, **24**, 596–601.

39. Kelley, L.A., MacCallum, R.M. and Sternberg, M.J. (2000) Enhanced genome annotation using structural profiles in the program 3D-PSSM. *J. Mol. Biol.*, **299**, 499–520.

40. Bertrand, D., Cooper, E., Valera, S., Rungger, D. and Ballivet, M. (1991) Electrophysiology of neuronal nicotinic acetylcholine receptors expressed in *Xenopus* oocytes following nuclear injection of genes or cDNA. In: *Methods in Neuroscience*, Conn, M. (ed.). Academic Press, New York, Vol. 4, pp. 174–193.

41. Saitou, N. and Nei, M. (1987) The neighbor-joining method: a new method for reconstructing phylogenetic trees. *Mol. Biol. Evol.*, **4**, 406–425.